Leonard Rusli
Research Engineer
Department of Mechanical and Aerospace Engineering,
The Ohio State University,
United States,
201 W. 19th Ave.
Columbus, OH 43210
e-mail: rusli.10@osu.edu

Anthony Luscher
Associate Professor
Department of Mechanical and Aerospace Engineering
The Ohio State University
201 W. 19th Ave.
Columbus, OH 43210
United States
e-mail: luscher.3@osu.edu

James Schmiedeler
Associate Professor
Department of Aerospace and Mechanical Engineering,
University of Notre Dame,
365 Fitzpatrick Hall,
Notre Dame, IN 46556,
United States
e-mail: schmiedeler.4@nd.edu

Analysis of Constraint Configurations in Mechanical Assembly via Screw Theory

The essential function of a mechanical assembly is the removal of degrees of freedom (DOF) to enable the transfer of load between two bodies. Assembly constraint features serve to provide this DOF removal, so their locations and orientations greatly affect the quality of an assembly as measured by its ability to resist relative motion between the parts. This paper addresses attachment-level design in which design decisions are made to establish the types, locations, and orientations of assembly features. The analysis methodology in this paper models assembly features such as point, pin, line, and plane constraints with equivalent first, second, and third order wrench systems. The set of relative motions to be evaluated is generated by composing from among these constraints a five-system pivot wrench combination to which a freedom screw motion is reciprocal. The effectiveness of each constraint to resist these motions is calculated as the ratio of the reaction forces at each resisting constraint to the input wrench magnitude. Based on these resistance values, multiple rating metrics are calculated to rate the overall assembly's performance in resisting the motion. This work represents the first tool available to analyze a constraint configuration's effectiveness to resist motion with a quantitative metric. Case studies are presented to demonstrate the utility of the analysis tool.
[DOI: 10.1115/1.4005622]

1 Introduction

Understanding mechanical assembly is a critical element in creating high quality product designs, and there are two levels of analysis of mechanical assembly to consider. The first, feature-level analysis, determines whether a single fastening feature is able to meet design requirements such as strength, stiffness, and fatigue limits. A wide range of quantitative metrics can be formulated based on the feature type and the specific intended application, so questions typically addressed in feature-level analysis include: How strong is the feature? How much force is required to assemble the feature? How much stress will the feature experience under a given load? Accordingly, there is a significant and well-recognized body of knowledge in areas such as bolted joint strength analysis and feature-level analysis of snap-fits.

In contrast, relatively little published research has examined the second, or attachment level of analysis, which assesses an assembly based on the overall constraint strategy. An attachment level constraint approach utilizes different features in the part geometry to remove degrees of freedom (DOF) rather than being focused on using individual fasteners (Fig. 1). Questions typically addressed in attachment-level analysis include: How effective is the overall constraint configuration in resisting loads? What would be the effectiveness of the constraint configuration after adding/removing specific features? How redundant is the constraint configuration? How significant is the role of a specific feature relative to others in resisting arbitrary loads? In most cases, the answers to these questions are not intuitive to the designer, especially in nonrectilinear and complex geometries under three-dimensional loadings. Even with simple geometries, assembly is often kinematically overconstrained, so the classical analysis of assembly forces and reactions is statically indeterminate, making quantitative metrics that rate the quality of an assembly as a whole difficult to formulate. As such, attachment-level design is currently performed in an ad-hoc manner. This motivates the development in this paper of a novel attachment-level analysis tool to quantify constraint effectiveness in assembly.

Relative to existing work, the greatest similarities to analysis of assembly constraint lie in analysis of robotic grasping and workpart fixturing, namely how contact interfaces that constrain motion are used to remove DOF. This paper specifically analyzes the removal of DOF via screw theory. Screws can be used to represent any spatial motion as a twist and any constraint that prevents motion as a wrench [1,2]. Waldron [3] and Hunt [4] applied screw theory to the constraint analysis of mechanisms, but its use in identifying form and/or force closure is more relevant to constraint analysis of assembly.

A number of binary tests to determine whether a set of unilateral point constraint configurations provides form closure have been proposed [5–9]. Binary tests, though, are not particularly useful for analyzing an assembly's performance because they do not give a quantitative rating of the constraint's effectiveness in resisting motion. As an alternative, the magnitude of internal forces induced by a known set of external wrenches can serve as a continuous metric to quantify robotic grasp stability [10,11]. Reaction force distribution is another method to determine grasp quality. Salisbury and Roth [12] identified finger configurations that allow complete immobilization of the gripped object and the associated internal forces that are acting on the object. Various methods for determining grasping forces to secure a grasp using elastic support models and/or minimum norm principles have followed this work [13–15]. All of these methodologies that calculate reaction forces, though, rely on stiffness values that are typically unknown in mechanical assembly problems. In addition, these methods usually assume a known clamping force, while assemblies are loaded by unknown external wrenches.

Contributed by the Mechanisms and Robotics Committee of ASME for publication in the JOURNAL OF MECHANICAL DESIGN. Manuscript received June 22, 2011; final manuscript received December 12, 2011; published online February 3, 2012. Assoc. Editor: Pierre M. Larochelle.

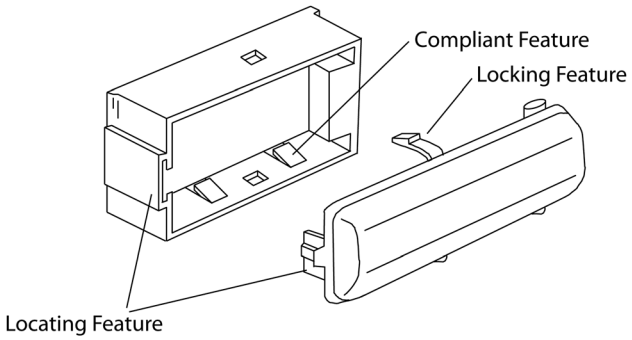

Fig. 1 Assembly constraint strategy using various features

Asada and By [16] and Ohwovoriole and Roth [17] used virtual work and the reciprocity equation to develop a continuous metric of the reciprocity level. This metric classifies the relationship between a screw and a wrench as contrary, reciprocal, or repelling, which refer to positive, zero, and negative virtual work in the metric, and thereby evaluates constraint effectiveness. Similar to this method, Bausch and Youcef-Toumi [18] developed a kinematic method to analyze the workholding condition by evaluating the motion stops corresponding to the reciprocal screw motions within a given fixture configuration. This method, which assumes only rigid, frictionless unilateral point constraints whose locations and orientations do not change, analyzes an overconstrained assembly configuration by identifying a set of weakly constrained motions using the reciprocity equation. It calculates a quantitative rating for each constraint based on the virtual displacement into that constraint. This is accomplished by calculating unique single-DOF motions, termed "freedom motions," each of which is reciprocal to a five-system wrench [19] formed by taking a corresponding combination of five unilateral and linearly independent constraints. The remaining constraints that are not part of the five system are then evaluated for their effectiveness in resisting the calculated motion by computing the motion's virtual displacement into the resisting constraint. A larger virtual displacement value indicates greater resistance to the particular motion.

Bozzo [20] analyzed constraint configurations in snap-fit assemblies by modifying Bausch and Youcef-Toumi's [18] algorithm to discretize planar contact into unilateral point constraints and to normalize the rating metric by the largest distance between two constraints in the configuration. His unilateral representation of planar contact and higher order constraints is similar to Ohwovoriole's and DeMeter's approach to planar contact [17,21,22]. The new models developed in this paper are motivated by two significant limitations in the constraint analysis methodology of Bausch and Youcef-Toumi [18] and Bozzo [20].

First, the approach is inadequate for mechanical assemblies because it does not address higher order contact (HOC) interfaces that remove more than one DOF per feature. Discretization of these HOC leads to several problems. For example, in Fig. 2, a pin constraint is discretized into eight unilateral point constraints that the methodology analyzes in combinations of five at a time.

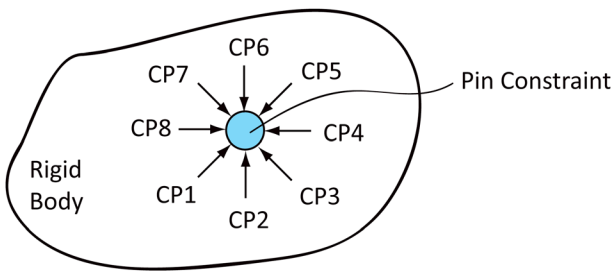

Fig. 2 Representing pin contact as many unilateral contacts

As the discretization resolution increases (employing n unilateral point constraints) to improve fidelity of the pin's representation, the number of evaluated combinations of five constraints increases in a factorial manner

$$C(n,5) = \frac{n!}{5!(n-5)!} \tag{1}$$

The computation time can become impractical once the number of constraints exceeds 44 (approximately 1 million possible combinations). Also, with five constraints considered in any one evaluation, only a subset of the discrete constraints that together represent the pin can be involved in any calculation. Failure to consider the full spectrum of the true pin constraint in every calculation throughout the analysis leads to inaccuracies, as illustrated in a later case study.

The second limitation is that the approach is not scalable because it treats pure translation entirely differently from all other motions. The effectiveness of the constraints to resist a motion is determined by computing the virtual penetration of the screw motion into the constraints. The virtual penetration vector is the projection of the instantaneous velocity vector of the screw motion onto the constraint normal direction. A larger velocity magnitude in the normal direction indicates more effective resistance provided by the constraint. For all finite pitch screws, the virtual penetration M due to an input rotation θ about the screw axis is

$$\text{Case1: } h \neq \infty, \quad M = (h\omega_u + (\omega_u \times R)).(-N) \tag{2}$$

where h denotes the pitch. For infinite pitch screws (pure translation), the value M is

$$\text{Case2: } h = \infty, \quad M = \mu_u.(-N) \tag{3}$$

where ω_u, μ_u, and N all have unit magnitude. Note that the maximum value of M for finite pitch screws grows proportional to the moment arm, and hence to part size, but the maximum value of M in pure translation is always one. This inconsistency makes comparison between finite pitch screw motions and pure translation impossible, thereby preventing proper identification of the most weakly constrained motion in the assembly.

This paper presents an attachment-level analysis tool that addresses these limitations by producing an accurate and consistent assembly model. The model and corresponding metric provide a physically meaningful and scalable rating scheme that a designer can use in developing better assemblies. The paper is organized around the methodology shown in Fig. 3. Section 2 discusses the kinematic screw equivalents used to model higher order assembly constraints (pins, lines, and planes) as wrench systems, addressing the first limitation. In Sec. 3, sets of motions allowed

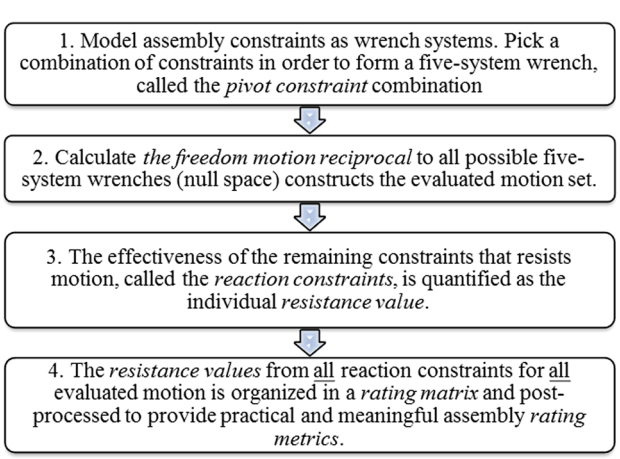

Fig. 3 Overall methodology algorithm

Table 1 Nomenclature

Terms	Definition
Assembly constraint configuration	The location and orientation of assembly constraint features that remove degree of freedom
CP	Point constraint
CPIN	Pin constraint of negligible depth
CLIN	Line constraint of finite length
CPLN	Plane constraint of finite area
Pivot constraints	Combination of constraints that compose a five-system wrench from which freedom motion is to be calculated
Evaluated motion set	The freedom motion reciprocal to the pivot constraint set that is unconstrained by the five-system pivot wrench
Reaction constraints	The constraints other than the pivot constraints that provide resistance to the evaluated motion set
Individual resistance value	The effectiveness measure of a single reaction constraint to resist a motion
Rating matrix	The matrix composed of individual resistance values organized in rows of evaluated motion set and columns of reaction constraints
Higher order constraint model	A model to represent pin, line, and plane constraints as equivalent wrench systems of order greater than one
Isolated reaction force model	A method to calculate the individual resistance value by representing the input load as force couple and calculating the reaction force at the reaction constraint

by taking combinations of the constraints are calculated using the reciprocity equation. Sec. 4 presents an isolated reaction force method to calculate the resistance quality of the assembly constraint configuration, addressing the second limitation. Lastly, Sec. 5 discusses several rating metrics that provide different ways to quantify the performance of an assembly, the utility of which is demonstrated by the three case studies in Sec. 6.

2 Modeling Assembly Constraints Using HOC Model

All assembly contact interfaces that remove DOF can be categorized as point, pin, line, or planar contacts, and guidelines are required to differentiate among these different categories. For example, when the area of planar contact is small enough compared to overall part dimensions, it may be more appropriate to consider it a point contact, and likewise for cases of short line contacts. The pin, line, and planar constraints are considered HOC because they remove more than one DOF, in contrast to point constraints that only remove one DOF. Constraints in assembly almost always involve HOC. This section describes the mathematical wrench constraint representations used to model such assembly contact interfaces.

Any spatial displacement can be represented as a screw displacement, and screws are commonly used to describe linear and angular velocities in 3D. A wrench is the reciprocal of a screw commonly used to describe forces and torques in 3D. Waldron [3] explored screw systems from first order to fifth order and described an exhaustive list of the special systems in each order. His nomenclature is used in this paper (Table 1). There are, though, two distinct differences between wrenches in screw theory and assembly contacts, which are especially applicable in line and plane constraints.

1. Wrenches in screw theory provide bidirectional (two-way) DOF removal, while assembly contact interfaces provide unidirectional (one-way) DOF removal. Assembly contact interfaces only resist motion in the "compressive" direction toward the contact surfaces. Although an assembly contact interface physically allows motion away from the constraint, it is assumed that the constraint configuration exerts reaction forces that always act to maintain contact throughout the infinitesimal motion. This is known as force closure [6]. Therefore, modeling the one-way assembly contact interfaces as a two-way wrench system arrives at the identical reciprocal screw motion. Moreover, if a constraint wrench set is a five-system, the reciprocal one-system screw is the same regardless of whether the five-system wrench is composed of one-way or two-way constraints.
2. Wrenches in screw theory always have infinite span length, while assembly contact interfaces are always finite in length and width. Both the finite line and the infinite line constraint set belong to the same wrench system. As a result, when the pivot wrench set contains at least two wrenches from the two-system spanned by the line contact, the reciprocal screw solution is invariant with respect to the line length. In the physical world, though, there is a point at which a line is short enough that it should be considered a single point constraint. This decision is driven by comparison between the line length and the longest distance between constraint points in the part. The above explanation can also be extended to apply to planar constraints (finite versus infinite plane).

A point contact is defined as a constraint that can exert a one-way reaction force along its normal direction in compression, but not in tension. A point constraint removes one DOF, namely translation in the normal direction. The equivalent wrench system is a single zero-pitch wrench coincident with the normal vector of the constraint. This is a one-system as shown in Eq. (4). Short line contact and small planar contact areas can also fall into this category, modeled as point constraints at their midpoint

$$\vec{s}_\alpha = \begin{bmatrix} 0 \\ \hat{\omega}_\alpha \end{bmatrix} \tag{4}$$

A pin contact is defined as a constraint that can exert a two-way reaction force in the radial direction. These reaction forces lie in the plane normal to the pin axis. A pin contact removes two DOF, namely translation along the two principal axes perpendicular to the pin axis. The equivalent wrench system is composed of all zero-pitch wrenches that are coplanar and intersecting at a point—the first-special two-system [3]. It is composed of a planar pencil of wrenches in the radial direction. The principal wrenches of this system are two perpendicular wrenches of zero pitch in the planar pencil [Eq. (5), Fig. 4]

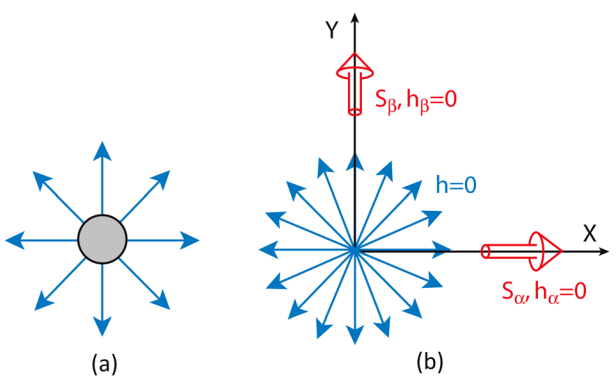

Fig. 4 (*a*) Pin constraint; (*b*) pin wrench equivalent

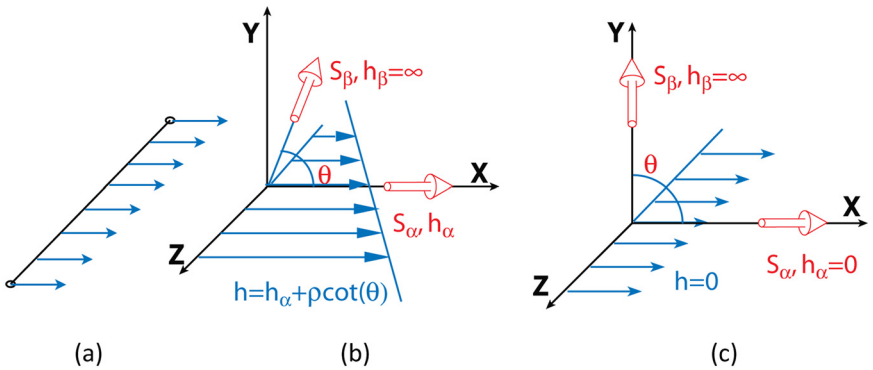

Fig. 5 (*a*) Line constraint; (*b*) second special 2-system wrench representation; (*c*) when $h_\alpha = 0$, $h_\beta = \infty$

$$\vec{s}_\alpha = \begin{bmatrix} 0 \\ \hat{i} \end{bmatrix}, \quad \vec{s}_\beta = \begin{bmatrix} 0 \\ \hat{j} \end{bmatrix} \tag{5}$$

Physical pin contact interfaces in assembly tend to be short in depth [z-direction in Fig. 4(*b*)] and are not designed to take moment loads. Therefore, they are mathematically modeled with zero depth and cannot exert reaction moments transverse to the pin axis. Hence, a pin constraint is different from a cylindrical constraint. The cylindrical constraint can exert reaction moments to restrain rotation transverse to the pin axis in addition to the two translational constraints. Since pin constraints only constrain translation in the radial direction, the constraint effectiveness is invariant with respect to radius.

A line constraint can be represented as a uniformly distributed unilateral constraint along a finite line, oriented normal to the mating surface. The equivalent wrench system is composed of an infinite number of parallel and coplanar zero-pitch wrenches [Fig. 5(*b*)] - the second-special two-system [3]. The general form of this special system is defined by a finite pitch wrench coincident with the local X-axis and an infinite pitch wrench oriented at an angle θ from the X-axis and lying in the XY plane. Equations (6) and (7) describe this special form

$$\vec{s}_\alpha = \begin{bmatrix} h_\alpha \omega_\alpha \hat{i} \\ \omega_\alpha \hat{i} \end{bmatrix}, \quad \vec{s}_\beta = \begin{bmatrix} \mu_\beta(\cos\theta\hat{i} + \sin\theta\hat{j}) \\ 0 \end{bmatrix} \tag{6}$$

$$h = h_\alpha + p\cot\theta \tag{7}$$

The line constraint is a special case when $h_\alpha = 0$ and $\theta = \pi/2$ The first principal wrench for this system is a zero-pitch wrench perpendicular to the line in the normal contact direction. The second principal wrench is an ∞-pitch wrench perpendicular to and intersecting the first principal wrench

$$\vec{s}_\alpha = \begin{bmatrix} 0 \\ \hat{i} \end{bmatrix}, \quad \vec{s}_\beta = \begin{bmatrix} \hat{j} \\ 0 \end{bmatrix} \tag{8}$$

A planar contact can exert a one-way reaction force in the direction normal to the plane. A plane constraint can be illustrated as a uniformly distributed unilateral constraint normal to a finite plane. The equivalent wrench system is composed of ∞^2 parallel zero-pitch wrenches [Eq. (9), Fig. 6]—the seventh-special three-system [3]. This system is defined by a finite pitch wrench coincident with the local X-axis, an infinite pitch wrench oriented at an angle θ from the X-axis and lying in the XY-plane, and another infinite pitch wrench oriented at an angle α from the X-axis and lying in the XZ-plane. The plane constraint is a special case when $h_\alpha = 0$ and $\theta = \alpha = \pi/2$, so the three principal wrenches create an orthogonal set. The first is a zero-pitch wrench normal to the plane. The second and third are ∞-pitch wrenches perpendicular to the first and to each other.

A curved line contact or a circumferential line contact can also be modeled as a plane contact because it spans a set of parallel but noncoplanar wrenches. Therefore, it is not equivalent to straight-line contact

$$\vec{s}_\alpha = \begin{bmatrix} 0 \\ \hat{i} \end{bmatrix}, \quad \vec{s}_\beta = \begin{bmatrix} \hat{j} \\ 0 \end{bmatrix}, \quad \vec{s}_\gamma = \begin{bmatrix} \hat{k} \\ 0 \end{bmatrix} \tag{9}$$

A single threaded fastener constraint can be modeled as a pin constraint with two additional opposite point constraints along the axis. Neglecting friction, the remaining DOF's are rotation around the three principle axes because a single fastener by itself does not effectively resist the moments about the two transverse axes. The equivalent wrench system is composed of ∞^2 infinite-pitch wrenches in all directions—the fifth-special three-system [3] defined by three orthogonal infinite pitch wrenches. Mathematically, it is equivalent to a spherical joint

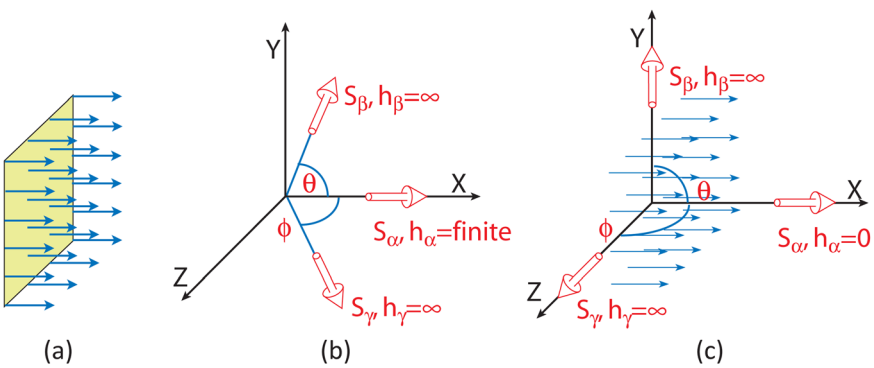

Fig. 6 (*a*) Plane constraint; (*b*) seventh special 3-system wrench representation; (*c*) when $h_\alpha = 0$, $h_\beta = h_\infty = \infty$

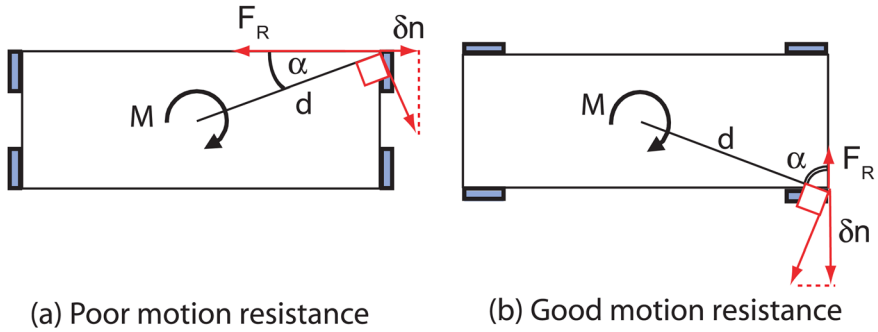

Fig. 7 Comparison of isolated reaction force versus virtual displacement model

$$s_\alpha = \begin{bmatrix} \hat{l} \\ 0 \end{bmatrix}, \quad \vec{s}_\beta = \begin{bmatrix} \hat{j} \\ 0 \end{bmatrix}, \quad \vec{s}_\gamma = \begin{bmatrix} \hat{k} \\ 0 \end{bmatrix} \tag{10}$$

Cylindrical contact found in hinges is modeled as a cylindrical constraint that removes four DOF, allowing rotation around the pin axis and translation along the axis. The equivalent wrench system is the third-special four-system [3]. A four-system is specified by its reciprocal two-system. The reciprocal of this four-system is a screw axis with any pitch coincident with the pin axis. This reciprocal screw is the third special two-system [Eq. (11)]

$$\vec{s}'_\alpha = \begin{bmatrix} 0 \\ \hat{l} \end{bmatrix}, \quad \vec{s}'_\beta = \begin{bmatrix} \hat{l} \\ 0 \end{bmatrix} \tag{11}$$

3 Evaluation of Motion Resistance Quality Using Isolated Reaction Force Model

The second step in the methodology is to solve for the freedom screw motion reciprocal to the five-system wrench formed by a combination of pivot wrenches. In order to satisfy the reciprocity relationship, the inner product between the pivot wrench set, arranged in a matrix, and the reciprocal screw motion must be zero [Eq. (12)]

$$\begin{bmatrix} \omega_{1x} & \omega_{1y} & \omega_{1z} & \mu_{1x} & \mu_{1y} & \mu_{1z} \\ \omega_{2x} & \omega_{2y} & \omega_{2z} & \mu_{2x} & \mu_{2y} & \mu_{2z} \\ \omega_{3x} & \omega_{3y} & \omega_{3z} & \mu_{3x} & \mu_{3y} & \mu_{3z} \\ \omega_{4x} & \omega_{4y} & \omega_{4z} & \mu_{4x} & \mu_{4y} & \mu_{4z} \\ \omega_{5x} & \omega_{5y} & \omega_{5z} & \mu_{5x} & \mu_{5y} & \mu_{5z} \end{bmatrix} \begin{bmatrix} \mu_{\mu_{6x}} \\ \mu_{\mu_{6y}} \\ \mu_{\mu_{6z}} \\ \omega_{\omega_{6x}} \\ \omega_{\omega_{6y}} \\ \omega_{\omega_{6z}} \end{bmatrix} = \begin{bmatrix} 0 \\ 0 \\ 0 \\ 0 \\ 0 \\ 0 \end{bmatrix} \tag{12}$$

The algorithm to compose the five-system wrench involves taking all possible combination of constraints and ensures that they form a linearly independent set. The reciprocal screw motion is obtained by solving for the 1-dimensional null space of the pivot wrench set of rank 5. This screw motion is calculated for each pivot wrench combination that is a linearly independent set. All of the solved screw motions are collected to be the set of motions whose resistance is to be evaluated.

The identified freedom screw motion is necessarily resisted by the remaining constraints called the reaction wrenches. Therefore, the third step in the methodology is to evaluate the resistance quality of these reaction constraints using the isolated reaction force model, which is conceptually similar to Yoshikawa's passive force closure model [6]. The effectiveness of each reaction constraint to resist a particular motion is measured by calculating the reaction force of the constraint, and smaller reaction forces correspond to better assembly quality. Therefore, this effectiveness measure provides the same information as the virtual displacement model, only inverted in scale.

In the example in Fig. 7, two sets of constraints with differing orientations are shown to resist the same motion, and the relative moment arm length d is identical in each case. The virtual penetration model calculates δn, which is proportional to $\sin\alpha$, where α is the angle between the moment arm and the constraint normal. The isolated reaction force model calculates F_R, which is inversely proportional to $\sin\alpha$. Therefore, case (a) yields a small virtual penetration and a large reaction force, indicating poor resistance, while case (b) yields a large virtual penetration and a small reaction force to indicate good resistance. Case (a) will induce a large reaction force, which will lead to unanticipated deformation of the constraining surface or possibly an early failure of a fastening feature. This is why the constraint configuration in case (b) is a better attachment strategy.

3.1 The Isolated Reaction Force Calculation.

The reaction forces are calculated by solving the vector static equilibrium equation involving the input wrench $\vec{L}$ and the constraining wrenches $\vec{C}_i$ with the origin located on the motion screw axis

$$\vec{L} + \vec{C} = \vec{0} \tag{13}$$

The constraining wrench $\vec{C}$ is composed of the pivot wrench $\vec{C}_{P1,P5}$ (five-system) and the reaction wrench $\vec{C}_R$ (one-system). Substituting this into the equilibrium equation and expressing in twist notation

$$\vec{L} + \left[\vec{C}_{P1,P5}, \vec{C}_R\right] = \vec{0} \tag{14}$$

$$\begin{bmatrix} \vec{\tau}_L \\ \vec{f}_L \end{bmatrix} + \begin{bmatrix} \hat{f}_{p1,5} \times \vec{r}_{p1,5} & \hat{f}_R \times \vec{r}_R \\ \hat{f}_{p1,5} & \hat{f}_R \end{bmatrix} \begin{bmatrix} \lambda_{1,5} \\ \lambda_6 \end{bmatrix} = \vec{0} \tag{15}$$

Note that the pivot wrench $\vec{C}_{P1,P5}$ is not necessarily composed of five constraints but will always have a set of five linearly independent wrenches (rank 5). When an HOC is part of the pivot wrench, less than five constraints may be involved. The system of linear equations described above is deterministic, and the intensity of the wrenches λ_1 through λ_6 can be found with a unique

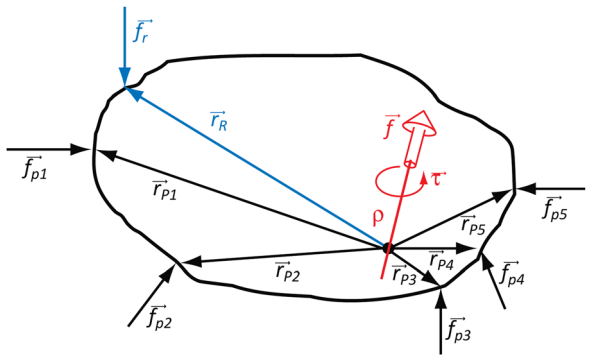

Fig. 8 Isolated reaction force model equilibrium

solution. Figure 8 illustrates the equilibrium of a rigid body under the input wrench and constraining wrenches.

The ratio between the magnitude of the reaction wrench λ_6 and the magnitude of the input wrench λ_i is taken as the individual rating of the effectiveness of the respective constraint with regard to the respective motion. The rating is called the resistance value RV

$$RV = \frac{\lambda_6}{\lambda_i} \tag{16}$$

Because it is a ratio, the resistance value is dimensionless. For simplicity, λ_i is set to be of magnitude 1. The value RV then can be interpreted as the required reaction force magnitude to resist a unit input wrench. Smaller resistance values mean that constraints are placed and oriented in a more effective and efficient manner. A motion that is close to being unconstrained will have a large reaction force, while a motion that is very effectively resisted will have a very small reaction force.

3.2 Input Wrench Magnitude Specification. One inherent problem with the virtual penetration model is that the input units for rotation differ from those for pure translation. The solution is to model the rotational component of the input wrench as a force couple instead of a concentrated moment (Fig. 9). The input wrench is modeled as force couple for two reasons. First, the magnitude of the input wrench should be scaled according to the size of the part, which is implied by the largest distance between constraints (in this case, C1 and C5). This will enable the model computation to be insensitive to part size. Second, in the context of real parts, any moment load applied on the part is always in the form of a force couple and never as a concentrated moment. Therefore, this approach is realistic.

The moment load induced by applying an input force couple λ_i at a distance d from the screw axis is $\lambda_i{*}d$. The moment arm length d is determined by measuring the longest perpendicular distance between the screw axis and the farthest constraint location. Alternatively, when part geometry data are available, the maximum distance between screw axis and the farthest point in the part can be used. This is the worst case scenario in the sense that $\lambda_i{*}d$ is the largest possible input load to be resisted. By modeling the input wrench as a force couple, the units for pure rotation, for combination of rotation and translation, and for pure translation are all consistent.

The second inherent problem in the virtual displacement model is the discontinuity of the input magnitude scale between finite and infinite pitch screw motions. This discontinuity can be resolved by dividing the screw motion pitch continuum from zero (pure rotation) to infinity (pure translation) into two ranges. In this approach, h_c is the critical pitch transition point at which the input magnitude (for both rotational and translational components) is equal.

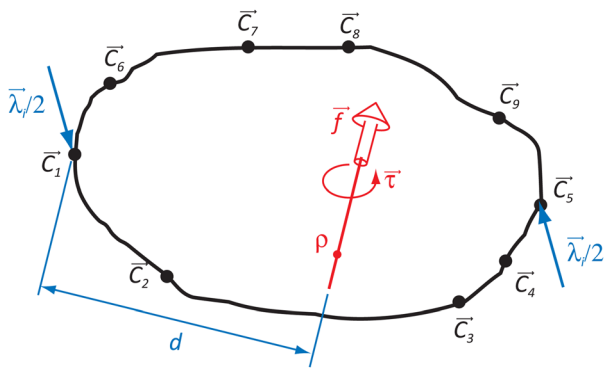

Fig. 9 The input wrench represented as a force couple

It is important to note the switch from screw to wrench notation at this point. A wrench is typically thought of as the reciprocal of a screw, but in this case, the input wrench is applied along the axis of the freedom screw motion, not reciprocal to it. In order to maintain the standard mathematical convention of screw theory, the pitch of the input wrench is adjusted as

$$h_w = \frac{1}{h_s} \tag{17}$$

where h_w is the pitch of the input wrench applied coincident to the motion screw with pitch h_s.

- **Case 1**: **Rotation-dominant motion**, defined by a motion with pitch

$$0 \le h_s \le h_c \tag{18}$$

or

$$\frac{1}{h_c} \le h_w \le \infty \tag{19}$$

The screw motion has a relatively small pitch compared to the critical pitch. The motion is called rotation-dominant because its rotational component magnitude is larger than its translational component magnitude. In this case, the input wrench magnitude is defined by the rotational component, namely the torque. The input wrench is generically defined by

$$\begin{bmatrix} \vec{\tau} \\ \vec{f} \end{bmatrix} = \begin{bmatrix} h_w \hat{f} + (\vec{\rho} \times \vec{f}) \\ \hat{f} \end{bmatrix} \tag{20}$$

where h_w is the pitch of the wrench and $\vec{\rho}$ is a point that lies on the wrench axis. In order to set the magnitude of the rotational component proportional to $\lambda_i d$, the translational component is multiplied by $\frac{\lambda_i d}{h_w}$ to give

$$\begin{bmatrix} \vec{\tau} \\ \vec{f} \end{bmatrix} = \begin{bmatrix} h_w \left(\frac{\lambda_i d}{h_w} \hat{f}\right) + \left(\vec{\rho} \times \left(\frac{\lambda_i d}{h_w} \hat{f}\right)\right) \\ \frac{\lambda_i d}{h_w} \hat{f} \end{bmatrix} \tag{21}$$

Simplifying, the input wrench magnitude is

$$\begin{bmatrix} \vec{\tau} \\ \vec{f} \end{bmatrix} = \lambda_i \begin{bmatrix} d\hat{f} + \frac{d}{h_w}(\vec{p} \times \hat{f}) \\ \frac{d}{h_w} \hat{f} \end{bmatrix} \tag{22}$$

or in terms of the motion screw pitch h_s

$$\begin{bmatrix} \vec{\tau} \\ \vec{f} \end{bmatrix} = \lambda_i \begin{bmatrix} d\hat{f} + h_s d(\vec{p} \times \hat{f}) \\ h_s d\hat{f} \end{bmatrix} \tag{23}$$

It can be observed that when $h_s = 0$ or $h_w = \infty$

$$\begin{bmatrix} \vec{\tau} \\ \vec{f} \end{bmatrix} = \begin{bmatrix} \lambda_i d\hat{f} \\ 0 \end{bmatrix} \tag{24}$$

This is a pure rotation screw. Therefore, the input wrench is a pure torque with magnitude $\lambda_i d$.

- **Case 2**: **Translation-dominant motion**, defined by a motion with pitch

$$h_c \le h_s \le \infty \tag{25}$$

or

$$0 \le h_w \le \frac{1}{h_c} \tag{26}$$

This screw motion has a relatively large pitch compared to the critical pitch. The motion is called translation-dominant because its translational component magnitude is relatively larger than the rotational component magnitude. In this case, the input wrench magnitude is defined by the translational component, namely the force. The input wrench is generically defined by

$$\begin{bmatrix} \vec{\tau} \\ \vec{f} \end{bmatrix} = \begin{bmatrix} h_w \vec{f} + (\vec{p} \times \vec{f}) \\ \vec{f} \end{bmatrix} \tag{27}$$

In order to set the magnitude of the translational component to λ_i, the equation is simply multiplied by λ_i to give

$$\begin{bmatrix} \vec{\tau} \\ \vec{f} \end{bmatrix} = \lambda_i \begin{bmatrix} h_w \hat{f} + (\vec{p} \times \hat{f}) \\ \hat{f} \end{bmatrix} \tag{28}$$

or in terms of the motion screw pitch h_s

$$\begin{bmatrix} \vec{\tau} \\ \vec{f} \end{bmatrix} = \lambda_i \begin{bmatrix} \frac{1}{h_s} \hat{f} + (\vec{p} \times \hat{f}) \\ \hat{f} \end{bmatrix} \tag{29}$$

It can be observed that when $h_s = \infty$ or $h_w = 0$

$$\begin{bmatrix} \vec{\tau} \\ \vec{f} \end{bmatrix} = \lambda_i \begin{bmatrix} (\vec{p} \times \hat{f}) \\ d\hat{f} \end{bmatrix} \tag{30}$$

This is a pure translation screw. Therefore, the input wrench is a pure force with magnitude λ_i.

Based on the magnitude formulation above, the critical pitch transition point, where the input wrench magnitude is equal, is determined to be $h_c = \frac{1}{d}$. At this critical pitch, the input wrench in both cases is equal to

$$\begin{bmatrix} \vec{\tau} \\ \vec{f} \end{bmatrix} = \lambda_i \begin{bmatrix} d\hat{f} + (\vec{p} \times \hat{f}) \\ \hat{f} \end{bmatrix} \tag{31}$$

Substituting the input wrench specification into Eq. (31), the equilibrium equations for cases 1 and 2, respectively, become

$$\lambda_i \begin{bmatrix} d\hat{f} + h_s d(\vec{p} \times \hat{f}) \\ h_s d\hat{f} \end{bmatrix} + \begin{bmatrix} \hat{f}_{P1,5} \times \vec{r}_{P1,5} & \hat{f}_R \times \vec{r}_R \\ \hat{f}_{P1,5} & \hat{f}_R \end{bmatrix} \begin{bmatrix} \lambda_{1,5} \\ \lambda_6 \end{bmatrix} = \vec{0} \tag{32}$$

$$\lambda_i \begin{bmatrix} \frac{1}{h_s} \hat{f} + (\vec{\rho} \times \hat{f}) \\ \hat{f} \end{bmatrix} + \begin{bmatrix} \hat{f}_{P1,5} \times \vec{r}_{P1,5} & \hat{f}_R \times \vec{r}_R \\ \hat{f}_{P1,5} & \hat{f}_R \end{bmatrix} \begin{bmatrix} \lambda_{1,5} \\ \lambda_6 \end{bmatrix} = \vec{0} \tag{33}$$

For simplicity, the equilibrium is set up with ρ as the origin, and hence, $\vec{\rho} = \vec{0}$. Simplifying further, the equilibrium equations for cases 1 and 2 become

$$\lambda_i \begin{bmatrix} d\hat{f} \\ h_s d\hat{f} \end{bmatrix} + \begin{bmatrix} \hat{f}_{P1,5} \times \vec{r}_{P1,5} & \hat{f}_R \times \vec{r}_R \\ \hat{f}_{P1,5} & \hat{f}_R \end{bmatrix} \begin{bmatrix} \lambda_{1,5} \\ \lambda_6 \end{bmatrix} = \vec{0} \tag{34}$$

$$\lambda_i \begin{bmatrix} \frac{1}{h_s} \hat{f} \\ \hat{f} \end{bmatrix} + \begin{bmatrix} \hat{f}_{P1,5} \times \vec{r}_{P1,5} & \hat{f}_R \times \vec{r}_R \\ \hat{f}_{P1,5} & \hat{f}_R \end{bmatrix} \begin{bmatrix} \lambda_{1,5} \\ \lambda_6 \end{bmatrix} = \vec{0} \tag{35}$$

Case 1 is represented in the region where $h_s < d$ in Fig. 10(*a*) and where $h_w > d$ in Fig. 10(*b*). In this rotation dominant motion, the input torque magnitude is set to one, and the input force is calculated with Eq. (34). Case 2 is represented in the region where $h_s < d$ in Fig. 10(*a*) and where $h_w < d$ in Fig. 10(*b*). In this translation dominant motion, the input force magnitude is set to one, and the input torque is calculated with Eq. (35). It can be observed that the input wrench magnitude is equal and continuous at the critical pitch $h_s = \frac{1}{d}, h_w = d$. Hence, the discontinuity problem in Bausch and Youcef-Toumi's [18] model is eliminated.

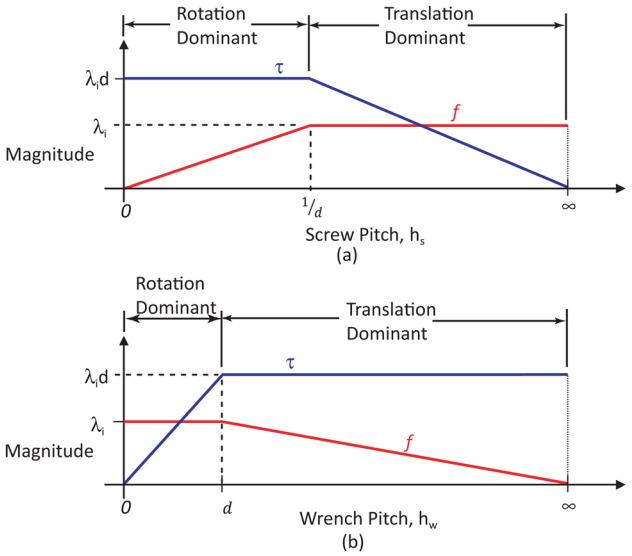

Fig. 10 Input wrench magnitude versus (*a*) screw pitch and (*b*) wrench pitch

3.3 Reaction Wrench Composition. The reaction wrench $\vec{C}_R$ is composed differently depending on the type of constraint, as it can be a point (one-system), pin (two-system), line (two-system), or plane (three-system). With the exception of the point reaction wrench, HOC reaction wrenches will be modeled as multiple point reaction forces at their optimal locations and orientations, which are defined as those providing motion resistance with the smallest possible reaction force for consistency with the minimum energy principle.

$\vec{P}$ the position vector of the constraint center coordinate. $\vec{R}$ is the vector between the constraint center coordinate and the point on the screw axis and is equal to $\vec{R} = \vec{P} - \vec{\rho}$. $\hat{N}$ is the unit normal vector of the reaction wrench orientation. The reaction wrench is defined as

$$\vec{C}_R = \begin{bmatrix} \vec{R} \times \hat{N} \\ \hat{N} \end{bmatrix} \tag{36}$$

After the pivot wrenches $\vec{C}_{P1,P5}$ are merged with the reaction wrench $\vec{C}_R$,, the equilibrium equation

$$\left[\vec{C}_{P1,P5}, \vec{C}_R\right][\lambda_i] = -\vec{L} \tag{37}$$

can be solved for the reaction force intensities λ_i. For cases in which the merged constraint wrench is rank-deficient (less than 6), the reaction wrench is linearly dependent to the pivot wrench system and therefore unable to resist the motion; its resistance value is set to infinity. Only the reaction force intensity λ_6 for the reaction wrench is used as the resistance value. Positive resistance values correspond to forward screw motion resistance, and negative resistance values correspond to backward screw motion resistance.

The magnitude of the resistance value, interpreted as a "load amplification" ratio, has a direct and practical design application. It is inversely proportional to the effectiveness of an individual

constraint, so smaller resistance values indicate that a constraint is more effective in resisting motion. Note that λ_6 is inversely proportional to its moment arm distance to the screw axis

$$\lambda_6 \sim \frac{1}{|\vec{r}_R|} \tag{38}$$

For a very short moment arm distance (the constraint is located very close to the screw axis), the reaction force approaches infinity. Contrasting this are larger moment arm distances (the constraint is located very far from the screw axis), although they have diminishing return in giving the reaction wrench a mechanical advantage. This desired and actual nonlinear behavior was not present in the virtual penetration method, where the rating is linearly proportional to its distance from the screw axis.

4 Assembly Performance Rating Metrics

The postprocessing of these individual resistance values begins with arranging them in a matrix, with the rows correspond to the motions, and the columns correspond to the constraints. For m evaluated motions and n evaluated constraints, the size of the rating matrix is $m \times n$. For each motion (row), there will always be a few constraints with infinite reaction forces. These represent either the set of pivot constraints to which the motion is reciprocal or any constraint that is linearly dependent to the pivot constraint set. They have infinite reaction forces because these constraints cannot do any work to resist the motion by the definition of reciprocity. Any constraint that is linearly independent from the pivot wrenches resists the motion and has a noninfinite value.

Table 2 shows a sample rating matrix with eight constraints (C_1 through C_8). The infinite values are caused by the constraints that are either the pivot constraints or constraints that are linearly dependent to the pivot constraints. The finite resistance values are the actively resisting constraints for the respective motion with the smaller this number is, the more effective resistance it provides.

In a commonly occurring over-constrained assembly, more than one constraint is involved in resisting any single motion. These constraints work together to share the load, and thereby improving resistance. While multiple constraints increase assembly performance in an additive manner, individual resistance values increase assembly performance when they decrease in value (reaction forces). This conflicting scale is resolved by taking the reciprocal sum to get the shared resistance value of a single motion

$$\frac{1}{\text{Shared Resistence}} = \sum_1^n \frac{1}{c_i} \tag{39}$$

To measure how well each motion is resisted, the shared resistance is calculated by the reciprocal sum of each row. The shared resistance value, like the individual resistance value, can be understood as a load amplification ratio. For example, a shared resistance value of 0.5 means that on average, the reaction force magnitude on the actively resisting constraints is 0.5 times the input load. Higher shared resistance values yield undesirable large reaction forces on the constraints, while lower shared resistance values yield desirable small, shared reaction forces on the constraints.

Finally, different rating metrics are developed to measure an assembly's performance from different design perspectives. The first measures the assembly's performance based on its capability to resist the most weakly constrained motion. This is an appropriate metric since an assembly is only as good as its weakest motion resistance. The sum of ratings for the most weakly constrained motion is called the weakest shared resistance (WSR) rating. The rating is calculated by

$$WSR = max(Shared\,Resistence_j) \tag{40}$$

where M is the rating matrix of size $m \times n$. In the sample rating matrix displayed in Table 2, the WSR is identified for motion 3 with a WSR value of 0.637. The identified most weakly constrained motion is specified in terms of the screw axis direction vector ω, a coincident point that lies on the motion screw axis ρ, and the pitch h. A tolerance of 10% of the WSR rating is applied to capture similarly rated motions.

The second measure, the mean shared resistance rating (MSR), characterizes the assembly's resistance quality toward general motion. Two constraint configurations may have identical WSR ratings, but their overall effectiveness (MSR) may not be identical. This is affected by how the rest of the motions (except the most weakly constrained) are resisted. This is rating is calculated by

$$\text{MSR} = \frac{\sum_1^n \text{Shared Resistenc } e_j}{m} \tag{41}$$

Similar to the WSR rating, the MSR rating can also be understood in terms of load amplification ratio in order to aid physical interpretation. In the sample rating matrix displayed in Table 2, supposing that only motion 1 through 6 is the evaluated set, the MSR value is average of the shared resistance column, which is 0.431.

There are two more rating metrics to observe the relative importance of individual constraints in a configuration. The third measure is the constraint active percentage (AP) rating, which is similar to one of Bozzo's [20] metrics. A constraint is considered inactive when its resistance value is infinite for a particular motion. A constraint can be inactive due to belonging to a pivot wrench or because its reaction force is negative (repelling screws according to Asada [16]). The AP value is calculated by computing the percentage of motions for which a particular constraint is active

$$AP_j = \frac{\#\,of\,(M_j \neq 0)}{m} \tag{42}$$

This rating metric gives a measurement of the uniqueness of the DOF removal provided by an individual constraint. The larger this rating is, the more unique this constraint is in removing a particular screw motion. The smaller it is, the more frequently this constraint acts redundantly with the other constraints. It is generally desirable for constraints in a configuration to share the load more uniformly, thereby increasing the overall capacity of an assembly

Table 2 Sample rating matrix

	C_1	C_2	C_3	C_4	C_5	C_6	C_7	C_8	Shared resistance
Motion 1	Inf	Inf	Inf	Inf	Inf	1.247	0.970	0.982	0.351
Motion 2	2.710	Inf	Inf	0.669	Inf	Inf	1.397	Inf	0.388
Motion 3	Inf	Inf	1.290	Inf	1.256	Inf	Inf	Inf	0.637
Motion 4	Inf	1.057	Inf	17.544	Inf	1.253	Inf	Inf	0.555
Motion 5	Inf	0.893	Inf	Inf	Inf	Inf	0.772	0.833	0.277
Motion 6	0.863	Inf	1.107	Inf	Inf	Inf	Inf	1.695	0.377
Motion …	…	…	…	…	…	…	…	…	…

to resist loads. Less active constraints are good candidates for elimination when reducing assembly constraints is a goal.

The fourth measure, the best resistance percentage (BRP), is the frequency of a constraint not only actively resisting motion, but also having the smallest resistance value in resisting a particular motion. The BRP is calculated by

$$\mathrm{BRP}_j = \frac{\#\ of\ (\min(M_j))}{m} \tag{43}$$

This rating metric is useful to identify the constraint that provides more significant resistance compared to the others that are active. Constraints with high BRP ratings tend to take up larger loads than usual and hence should be prioritized in design for better stiffness, robustness, and tolerance.

5 Case Studies

Three case studies are presented. The first demonstrates the analysis tool in a general sense on an exactly constrained object. The second emphasizes the improvement in modeling constraints using HOC, and the third highlights the scalability of the approach when modeling an input wrench as a force couple and considering both finite-pitch and translational motions.

5.1 Exactly Constrained Design Chair Case Study. The purposes of this case study are two-fold. It demonstrates the agreement between the analysis results and theoretical kinematic principles for an exactly constrained body in 3D space, and it presents the interpretations of various rating metrics in their respective contexts. The exactly constrained design (ECD) chair is a three-legged stool with seven point constraints (Fig. 11). The foot of each leg is a sphere, with the first leg constrained by an inverted trihedral (CP1, CP2, CP3), the second by a V-groove (CP4, CP5), and the third by point-on-plane contact (CP6). The seventh point constraint, CP7, is located on top of the stool.

The results are provided in Table 3. The load amplification ratios are 5.236 (from WSR rating) and 1.404 (from MSR rating). Therefore, the reaction force of the constraints to resist the most weakly constrained motion is about five times the input load. The MSR rating shows that on average, considering all of the evaluated motions, the reaction force is 1.404 times the input load. An exactly constrained assembly tends to have fewer constraints

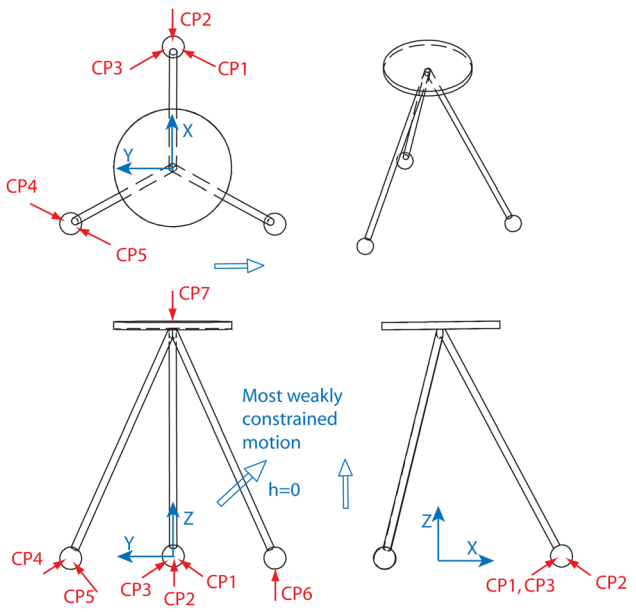

Fig. 11 ECD geometry constraint configuration and WSR motion

Table 3 ECD geometry analysis results

Overall rating metric		
WSR = 5.236		
MSR = 1.404		
Screw axis direction, pitch (h) = 0.000		
0.000	− 0.708 Screw axis coincident point	0.706
− 2.000 Constraint	1.724 AP (%)	1.731 BRP (%)
CP1	14.30	14.30
CP2	14.30	14.30
CP3	14.30	14.30
CP4	14.30	14.30
CP5	14.30	14.30
CP6	14.30	14.30
CP7	14.30	14.30

Table 4 Partial rating matrix for ECD geometry

	C_1	C_2	C_3	C_4	C_5	C_6	C_7
Motion …	…	…	…	…	…	…	…
Motion 13	Inf	Inf	Inf	Inf	0.724	Inf	Inf
Motion 14	Inf	Inf	Inf	2.494	Inf	Inf	Inf
Motion 15	Inf	Inf	1.339	Inf	Inf	Inf	Inf
Motion 16	Inf	Inf	Inf	Inf	Inf	Inf	5.236
Motion 17	Inf	Inf	Inf	Inf	Inf	1.855	Inf
Motion …	…	…	…	…	…	…	…

resisting the motion and hence larger reaction forces at the support points. This is mentioned by Slocum [23] as the trade off of gaining precision of position by sacrificing load carrying capability. Because this is an exactly constrained assembly, all constraint active percentage (AP) is equally distributed.

In order to make more detailed observations, a portion of the rating matrix is provided in Table 4. There are 21 possible combinations in choosing 5 of the 7 constraints as pivot constraints. Each combination is linearly independent because of the nature of exact constraint. Because of the bi-directional nature of each screw motion, the number of pivot constraints to be computed doubled. This results in 42 unique screw motions evaluated in the algorithm.

It can be observed that for each motion (row), there are at least five constraints incapable of resisting the motion because they are the pivot constraint set (e.g., for motion #17, CP1–CP5). The other remaining two constraints must actively resist the screw motion, or there will be unconstrained motion (e.g., for motion #17, CP6 or CP7). It can be observed that for each motion, one of the remaining two constraints resists the forward motion while the other resists the backward motion. Any constraint/wrench that is linearly dependent to the pivot wrenches is unable to resist the reciprocal motion; therefore, no six of these constraints/wrenches may belong to the same linear complex; otherwise, total restraint is not achieved. This shows that the assembly geometry in this case study, which has seven linearly independent point constraints, is an exactly constrained one, or deterministic. This example shows that the methodology is accurate and demonstrates exact constraint kinematics of a body constrained by seven unilateral point constraints such as shown by Lakshminarayana [19].

5.2 End Cap Assembly HOC Case Study. The objective of this case study is to demonstrate HOC modeling and study its effectiveness compared to discretizing the HOC into many point

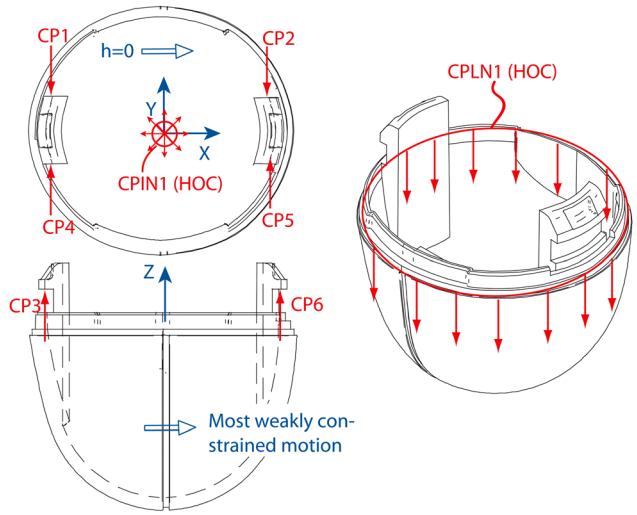

Fig. 12 Endcap geometry and constraint configuration

constraints (non-HOC model). The end cap is part of an actual assembly of a medicine spray housing (Fig. 12). The locking features are two cantilever snap-fits located symmetrically at the lips of the end cap. The part is also constrained by a pin constraint and a plane constraint, both provided by the stepped lip mating interface.

The circular line contact that constrains the end cap in the negative z-direction is a wrench system equivalent of a circular plane constraint and is treated as such (CPLN1). The curved line contact that constrains the end cap in the radial direction is a wrench system equivalent of a pin constraint (CPIN1). The line contact between the snap-fit retention face and the mating part does not extend to the overall part length and is relatively short in length. This line contact will be modeled as a point contact (CP3, CP6). Modeling an HOC as a lesser degree constraint (in this case, downgrading a line to a point) makes the results more conservative. There is an additional combination of pivot constraints that adds more motions to consider. Taking this approach will make the analysis more conservative, which means that the overall rating will be slightly underrated.

The analysis yield a WSR rating for the assembly is 1.000. Most of the constraints are located at the edges of the part. It is common for zero and infinite pitch screw axes to pass through constraint points or be coincident with constraint directions because constraints tend to act as pivot points. In these cases, the input wrench force couple moment arm is equal to the moment arm of the resisting constraints, yielding a resistance value of 1. The most weakly constrained motion is a pure rotation about an axis that passes across both snap-fit locks (noted in Fig. 12). This is also verified through physical examination of the assembly. The end cap assembly exhibits symmetry in the most weakly constrained motion set with respect to screw axis direction as is expected due to the part geometry. The plane contact is shown to be more active in resisting motion as well as being the most important reaction constraint. This is typical of HOC. The possibility of an HOC to resist arbitrary motion is higher because they remove more DOF.

In order to observe the accuracy and computational efficiency of the higher order constraint (HOC) modeling, a comparative study between the HOC model and a non-HOC model is done. The non-HOC model discretized the plane into eight parallel point constraints with the normal direction in the negative z-direction (CP9–CP16) and the pin constraint into 8-point constraints with the normal vector directed to the center of the pin (CP17–CP24).

Table 5 summarizes the comparison results, showing that the number of combinations the non-HOC model needs to compute is much higher, leading to longer computation time. The number of unique motions evaluated is significantly less after removal of duplicates and linearly dependent combinations. This reduction is clearly higher in non-HOC model because it involves combining constraints that belong to the same HOC.

Table 5 Comparison of HOC vs. non-HOC model analysis results

	HOC model	Non-HOC model
Initial number of combinations	210	42504
Linearly independent combination sets	20	282
Unique motion evaluated	12	148
Computation time (s)	0.36	12.5
WSR	1.000	0.546
MSR	0.615	0.379

Table 6 Example of pseudo-redundancy effect in non-HOC model

	Screw axis direction		
	− 0.269	− 0.963	0.000
	Screw axis coincident point		
Motion (Pitch = 0.000)	− 0.587	0.164	0.000
Pivot constraints	CP1, CP2, CP5 CP9, CP23		
Active reaction constraints	CP10, CP11, CP12, CP13, CP14, CP15, CP16		

A closer look reveals that many of these motions' pivot constraint sets contain only one or two wrenches that are taken from the HOC of which they are members. Because they only represent part of the HOC, these are "fictitious" motions that the pivot constraints would not allow for that particular geometry. These motions also tend to be rated better because the resistance can come from other discretized point constraints that do not belong to the resisting constraints but from the pivot constraints. For example, one of the evaluated motions done without the HOC model is specified in Table 6.

CP9 is shown as one of the pivot constraints, and the motion is actively resisted by CP10–CP16, but CP9–CP16 belongs to the pivot constraint feature, namely the planar constraint around the lip of the end cap. Therefore, this motion is reciprocal to *and* actively resisted by the *same* constraint feature. This is inconsistent with the principle that a wrench reciprocal to a screw motion cannot do any work, or in this case, resist the motion. This motion is not a valid motion to evaluate and will skew the rating of the assembly. This is called the pseudoredundancy effect. This is why the non-HOC model is falsely rated better as demonstrated by this example. The HOC model eliminates the possibility of such combinations.

In addition, due to the significantly higher number of constraint combination to process, the computational time of the non-HOC model is one-to-two orders of magnitude more than HOC model. Hence, the HOC model offers greater efficiency as well as greater accuracy.

5.3 Generic Cube Scalability Case Study. The generic cube is a 25.4 mm cube with point constraints at various locations on all faces (Fig. 13). The objective of this case study is to demonstrate the consistency provided by the isolated reaction force model. One way to demonstrate this capability is by observing the results as the constraint configuration is uniformly scaled up in size. The isolated reaction force couple model should resolve the scalability issues as well as the discontinuity between rotation and translation scaling that occur in other models. A scale factor of 2 is applied to the cube.

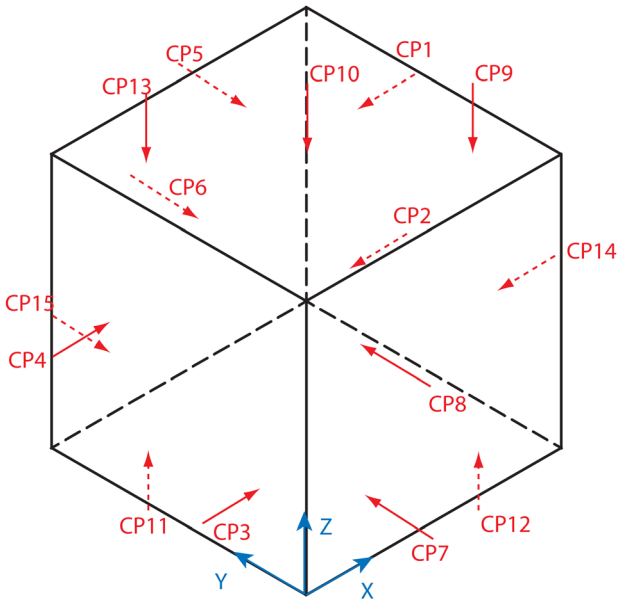

Fig. 13 Generic cube constraint configuration

Table 7 Cube scalability test result comparison

	Cube (Scale = 1)	Cube (Scale = 2)	Percentage difference
WSR	0.200	0.189	− 5%
MSR	0.486	0.473	− 3%

The results in Table 7 show that the WSR and MSR ratings for the assembly differ by 3–5%. In looking at the rating matrix, the shared resistance for motions with zero or infinite pitch is exactly identical between the two scaled models. This shows that by modeling the input load as a force couple with a properly scaled input moment arm, the resistance value stays constant for the pure rotation ($h = 0$) motions. In the case of infinite pitch motions (pure translation), the shared resistance stays constant because the resistance value depends only on the orientations of the constraints and not their positions. The orientations of the constraints do not change due to the scaling.

The WSR and MSR results differ by 3–5% due to the shift in screw motion with finite pitches when the cube is scaled. For cases in which the pitch is neither zero nor infinite, there is a slight variation due to the minimal shift in the screw motion pitch. In order to maintain reciprocity, the translational component $h\vec{\omega}$ of the screw motion must be scaled by 2, while the rotational component $\vec{\omega} \times \vec{R}$ is not. This is manifested in the pitch h being scaled by 2. Although the shared resistance rating is slightly different for finite pitch motions, the difference in assembly rating is minimal (3–5%). In addition, comparing the shared resistance values of the cubes with scale factors of 1 and 2 shows that there is no noticeable difference in the pattern of the motion resistance ratings.

The scalability test case study demonstrated that the analysis tool achieved far greater consistency and scalability compared to previous models by using the isolated reaction force couple model. The motion shift for nonzero and noninfinite pitch motions can be explained by understanding the change in the screw motion geometry, which happens when pivot constraint relative positions are modified.

6 Conclusion

There is a need for a practical assembly constraint analysis tool that provides a quantitative metric of assembly quality and is able to analyze assembly design at the attachment strategy level. This paper developed a model and methodology for analyzing an assembly constraint configuration that is able to:

- Accurately and efficiently model contact interfaces such as point, pin, line, and plane contacts in mechanical assemblies with equivalent wrench/screw systems using the HOC model. This eliminates the need to discretize HOC contact interfaces into many point constraints, which is both inaccurate and inefficient.
- Evaluate constraint effectiveness based on the reaction forces to resist motion. The isolated reaction force model consistently computes the resistance for rotation-dominant motion as well as translation-dominant motion. A scheme to model the input wrench as a force couple and to separate the motion into two different cases depending on the pitch is able to resolve the pitch discontinuity problem.
- Provide resistance values and rating metrics that can be interpreted as load amplification ratios, which quantify the magnitude of the reaction force generated for a given input load. The load amplification ratio produced by this model has direct design applications and better physical significance in the context of a real assembly compared to virtual displacement rating. The rating metrics are the overall measure of an assembly's effectiveness to resist motion and its effectiveness in removing DOF.

7 Limitations and Future Work

The rigid body assumption implies there is no deformation causing a change in the constraints' locations and/or orientations. Any such deformation would change both the evaluated screw motion set and the resistance quality of that constraint. Constraints also have different stiffness in different directions. Stiffer constraints tend to carry more load. Therefore, the actual distribution of reaction forces among the constraints is not only dependent on the location and orientation of each constraint, but also the relative stiffness of the constraints. The next step to improve this assembly tool is to incorporate stiffness into the model by weighing the resistance values in the rating matrix in proportion with their relative stiffness.

Due to the frictionless assumption, the methodology tends to underestimate the resistance quality of an assembly and is therefore conservative. However, good practice and design codes often require that friction be ignored in the design of joints so this assumption is often appropriate.

There is a decision continuum whether the size of a line or plane is large enough to be considered an HOC, or small enough to be considered a point constraint. Not using HOC in cases where lines and planes are relatively short results in a more conservative analysis and tends to underrate an assembly. There is a need for further study in establishing a guideline for this decision. Such a guideline might be determined based on a ratio between the relative length of a line or plane versus the overall size of the part. Since stiffer contact interfaces maintain their shape better than more compliant ones, constraint stiffness should be included in the guideline too.

References

[1] Ball, R. S., 1990, *A Treatise on the Theory of Screws*, Cambridge University Press, Cambridge, UK.
[2] Reuleaux, F., 1876, *The Kinematics of Machinery*, MacMillan, London.
[3] Waldron, K., 1996, "The Constraint Analysis of Mechanisms," J. Mech., **1**, pp. 101–114.
[4] Hunt, K. H., 1978, *Kinematic Geometry of Mechanisms*, Oxford University Press, New York.
[5] Rimon, E., and Burdick, J., 1996, "On Force and Form Closure for Multiple Finger Grasps," *Proceedings of the 1996 IEEE International Conference on Robotics and Automation*, Minneapolis, MN, pp. 1795–1800.
[6] Yoshikawa, T., 1996, "Passive and Active Closures by Constraining Mechanisms," *Proceedings - IEEE International Conference on Robotics and Automation*, Vol. 2, pp. 1477–1484.
[7] Shapiro, A., Rimon, E., and Burdick, J. W., 2001, "Passive Force Closure and its Computation in Compliant-Rigid Grasps," *IEEE International Conference on Intelligent Robots and Systems*, Vol. 3, pp. 1769–1775.
[8] Nguyen, V., 1988, "Constructing Force-Closure Grasps," Int. J. Robot. Res., **7**(3), pp. 3–16.

[9] Adams, J. D., and Whitney, D. E., 1999, "Application of Screw Theory to Constraint Analysis of Assemblies of Rigid Parts," *Proceedings of the IEEE International Symposium on Assembly and Task Planning*, Porto, Portugal, pp. 69–74.
[10] Trinkle, J. C., 1992, "A Quantitative Test for Form Closure Grasps," *Proceedings of the 1992 IEEE/RSJ International Conference on Intelligent Robots and Systems, Raleigh, NC*, pp. 1670–1677.
[11] Chen, Y.-C., and Walker, I. D., 1994, "Visualization of Form-Closure and Force Distribution for Grasping Solid Objects," *Proceedings of the IEEE International Conference on Systems, Man and Cybernetics*, Vol. 1, pp. 154–159.
[12] Salisbury, J. K., and Roth, B., 1983, "Kinematic and Force Analysis of Articulated Mechanical Hands," ASME J. Mech., Transm., Autom. Des., **105**(1), pp. 35–41.
[13] Kerr, J., and Roth, B., 1986, "Analysis of Multifingered Hands," Int. J. Robot. Res., **4**(4), pp. 3–17.
[14] Dai, J. S., and Kerr, D. R., 1996, "Analysis of Force Distribution in Grasps Using Augmentation," J. Mech. Eng. Sci., **210**(3), pp. 15–22.
[15] Wang, M. Y., and Pelinescu, D. M., 2003, "Contact Force Prediction and Force Closure Analysis of a Fixture Rigid Workpiece With Friction," ASME J. Manuf. Sci. Eng., **125**(2), pp. 325–332.
[16] Asada, H., and By, A. B., 1985, "Kinematic Analysis of Workpart Fixturing for Flexible Assembly With Automatically Reconfigurable Fixtures," IEEE J. Rob. Autom., RA-1(2), pp. 86–94.
[17] Ohwovoriole, M. S., and Roth, B., 1981, "An Extension of Screw Theory," ASME J. Mech. Des., **103**, pp. 725–735.
[18] Bausch, J. J., and Youcef-Toumi, K., 1990, "Kinematic Methods for Automated Reconfiguration Planning," *Proceedings 1990 IEEE International Conference on Robotics and Automation, Cincinnati, OH*, pp. 1396–1401.
[19] Lakshminarayana, K., 1978, "Mechanics of Form Closure," ASME Paper 78-DET-32, New York.
[20] Bozzo, T., 1997, "A Constraint Rating Scheme for Snap-fit Assemblies," M.S. thesis, The Ohio State University, Columbus, OH.
[21] DeMeter, E. C., 1993, "Selection of Fixture Configuration for the Maximization of Mechanical Leverage," *Proceedings of the 1993 ASME Winter Annual Meeting*, New Orleans, LA, Vol. 64, pp. 491–506.
[22] DeMeter, E. C., 1994, "Restraint Analysis of Fixtures Which Rely on Surface Contact," ASME J. Eng. Ind., **116**(2), pp. 207–215.
[23] Slocum, A. H., 1992, *Precision Machine Design*, Prentice-Hall, New Jersey.